Environment Canada

Environnement Canada

National Water Research Institute

Institut National de Recherche sur les Eaux

VELOCITY DISTRIBUTIONS UNDER FLOATING COVERS

by

Y. L. Lau

VELOCITY DISTRIBUTIONS UNDER FLOATING COVERS

by

Y. L. Lau

Environmental Hydraulics Section
Hydraulics Division
National Water Research Institute
Canada Centre for Inland Waters
Burlington, Ontario

August 1981

Abstract

The k-ε turbulence model has been used to calculate the velocity distributions for a large number of channel flows with different top and bottom boundary roughnesses. The resulting distributions are used to review the standard procedures for stream gauging of ice-covered flows. It is found that the average of the velocities at two-tenths and eight-tenths of the depth is indeed very nearly equal to the overall mean velocity. Examination of the velocity profiles shows that the profiles deviate from the logarithmic distribution for about 40 percent of the flow depth. Other flow properties, such as the location of the maximum velocity and the mean velocities in the top and bottom layers, are also examined.

Résumé

On a utilisé le modèle de turbulence k-ε pour calculer la distribution des vitesses d'un grand nombre d'écoulements en canal présentant différentes rugosités limites de surface et de fond. On utilise les distributions résultantes pour analyser les méthodes normales de jaugeage des écoulements sous une couverture de glace. On constate que la moyenne des vitesses aux deux dixièmes et aux huit dixièmes de la profondeur d'un cours d'eau est en fait très près de la vitesse moyenne globale. L'étude des distributions de vitesses montre que ces distributions s'écartent de la distribution logarithmique sur environ 40 pour cent de la profondeur du cours d'eau. On analyse également les autres propriétés de l'écoulement, comme le point où la vitesse est maximale et les vitesses moyennes dans les couches de surface et de fond.

Management perspective

River discharges under ice cover, as estimated by gauging practices, are very difficult to verify. In this report, flow under ice covers has been investigated theoretically and experimentally. The results confirm that velocity measurements taken at 0.2 and 0.8 of the water channel depth give velocities for which the average is always very close to the true mean velocity.

Engineers can therefore utilize river flows under ice as determined by this survey method with confidence. Winter surveys should adopt the procedure as standard.

T. Milne Dick

Chief, Hydraulics

Perspective de gestion

Le débit d'une rivière sous une couverture de glace, estimé par les méthodes de jaugeage, est très difficile à vérifier. Dans le présent rapport, on présente les résultats d'une étude théorique et expérimentale de l'écoulement sous une couverture de glace. Ces résultats permettent de confirmer que les vitesses mesurées à 0,2 et 0,8 de la profondeur d'eau du canal donnent une moyenne qui est toujours trés près de la vitesse moyenne vraie.

Les ingénieurs peuvent donc utiliser sans crainte les débits de rivières obtenus par cette méthode d'estimation. Pour les estimations effectuées en hiver, on devrait adopter cette méthode.

Chef de l'Hydraulique

T. Milne Dick

TABLE OF CONTENTS

Introduction

Although stream gauging techniques for free surface flows have long been established and are to some extent supported by theory, the same is not true for stream gauging in flows under ice cover. For ice-covered rivers, the U.S. Geological Survey recommends averaging the velocities at 0.2 and 0.8 depths as for free surface flows or, when the depth is less than about 60 cm, obtaining the velocity at mid-depth and applying a correction coefficient of 0.88. Essentially the same procedure is used by the Water Survey of Canada. While this procedure might have been developed with the aid of some field data, it really has no theoretical basis and it is not certain how correct it may be over a variety of different flow conditions.

Many methods have been proposed for calculating the flow between covers with different roughnesses (Pratte, 1979). Nearly all of these methods involve the division of the flow into two layers which are separated by the line of maximum velocity, and the assumption of logarithmic velocity distribution in each layer. Recently, the k-ε turbulence model has been applied to study open-channel flows (Rastogi and Rodi, 1978) as well as the effects on flow distribution and mixing properties brought about by ice covers (Lau and Krishnappan, 1981). Model predictions for open-channel flows have been verified by Rodi (1978). Good comparisons with model predictions have also been obtained by this author in flows under floating covers and an example is given in Fig. 1 (symbols are defined in Fig. 2). The complete results are being summarized and will be published in a separate article.

In this article, the turbulence model has been used to calculate the velocity distributions for a large number of flows under a variety of conditions. The results are used to review the stream gauging procedure mentioned previously and to examine some of the flow properties which are important in the development of many of the equations for ice-covered flow.

The k-ε turbulence model

A very brief review of the turbulence model will be given here. Details of the derivation of the equations are given by Rodi (1978). The procedures used in the calculation of two-dimensional channel flows are explained by Lau and Krishnappan (1981).

Basically, the model involves the solution of the equations of continuity, momentum and the transport equations for the kinetic energy of turbulence k and its rate of dissipation ε. For two-dimensional channel flow, these equations can be written as:

$$[1] \qquad \frac{\partial u}{\partial x} + \frac{\partial v}{\partial y} = 0$$

$$[2] \qquad \frac{\partial u^2}{\partial x} + \frac{\partial uv}{\partial y} = \frac{\partial}{\partial y}\left(\nu_t \frac{\partial u}{\partial y}\right) + gS$$

$$[3] \qquad \frac{\partial uk}{\partial x} + \frac{\partial vk}{\partial y} = \frac{\partial}{\partial y}\left(\frac{\nu_t}{\sigma_k} \frac{\partial k}{\partial y}\right) + G - \varepsilon$$

$$[4] \qquad \frac{\partial u\epsilon}{\partial x} + \frac{\partial v\epsilon}{\partial y} = \frac{\partial}{\partial y}\left(\frac{\nu_t}{\sigma_\epsilon}\frac{\partial \epsilon}{\partial y}\right) + C_1 \frac{\epsilon}{k} G - C_2 \frac{\epsilon^2}{k}$$

in which u and v are the velocity components in the x and y directions respectively. x is measured along the channel bed and y is measured perpendicular to the x axis in the vertical plane (see Fig. 2). S is the slope, g is the gravitational acceleration and σ_k, σ_ϵ, C_1 and C_2 are empirical constants. G is the turbulent energy production due to mean motion given by

$$[5] \qquad G = \nu_t \left[\left(\frac{\partial u}{\partial y}\right)^2 + 2\left(\frac{\partial v}{\partial y}\right)^2\right]$$

and ν_t is the turbulent kinematic viscosity which is related to k and ϵ by

$$[6] \qquad \nu_t = C_\mu \frac{k^2}{\epsilon}$$

in which C_μ is an empirical constant.

Besides the use of the Boussinesq eddy viscosity concept, the main assumptions used in formulating this model are that the turbulence structure is governed by two characteristic parameters k and ϵ and that the expressions for the diffusion of k and ϵ can be written as gradient terms. As the assumptions involve only the turbulence structure, the values for the empirical constants should be the same regardless of the type of flow. Launder and Spalding (1974) tested the model with a variety of flows such as flows in pipes, channels, mixing layers, jets and wakes, and determined the values of the constants as follows:

$c_\mu = 0.09$; $\sigma_k = 1.00$; $\sigma_\varepsilon = 1.30$; $C_1 = 1.43$ and $C_2 = 1.92$.

To apply the model, the flow depth H, unit discharge q, and the equivalent sand roughnesses of the bottom and top boundaries K_1 and K_2 are specified. From the asymptotic solution of the model equations, one can obtain the velocity distribution when the flow is uniform, as well as the slope S required for uniform flow. Using an iterative process, one can also find out, for a particular discharge, bed slope and roughnesses K_1 and K_2, what the flow depth has to be for uniform flow. It should be mentioned that the model is applicable for developing flows and flows receiving jet discharges etc. but is applied here to calculate the simplest case of uniform flow.

The boundary condition for the velocity component u requires that, at the grid points closest to either wall, the velocity satisfies the universal law of the wall

$$[7] \qquad \frac{u}{u_*} = \frac{1}{\kappa} \ln \left(E \frac{u_* y_w}{\nu} \right)$$

in which u_* is the shear velocity; κ is the Von-Karman constant; ν is the kinematic viscosity of the fluid; y_w is the distance of the nearest grid point from the solid boundary; and E is a roughness parameter.

$$[8] \qquad E = 9.0 \qquad \text{for smooth walls, i.e. } K = 0.$$

$$[9] \qquad E = e^{\kappa B_s} \nu/u_* K \qquad \text{for rough walls.}$$

B_s is an empirical expression which fits the experimental relationship obtained by Nikuradse covering the smooth-turbulent, transitional and fully rough flow ranges (see Yalin, 1972). For fully rough flow B_s takes on the well known constant value of 8.5.

A comparison of the model prediction with the measured velocity profile in a flow with artifically roughened boundaries is given in Fig. 1. The model inputs were:

$q = 304.9\ cm^2/s$; $H = 8.92\ cm$; $K_1 = 0.7\ cm$ and $K_2 = 0.1\ cm$.

The predicted velocity distribution compares very well with the measured distribution. The predicted slope of 0.0017 for uniform flow is slightly higher than the measured slope of 0.0014.

Selection of flow variables

In this study the velocity distributions for a large number of flows between covers with different roughnesses are to be examined. Therefore, it is advantageous to use a dimensional analysis of the problem as a guide to the selection of flow variables.

The shape of the velocity distribution in a channel with a floating cover depends on the flow depth H; the unit discharge q or mean velocity U; the top and bottom roughnesses and the kinematic viscosity of the fluid. Any other variable such as the distance to the point of maximum velocity, y_{max}, or the velocity at mid-depth, $u_{0.5}$, etc. should depend only on the aforementioned variables. Therefore, one can write:

$$[10] \qquad \frac{y_{max}}{H} = f\left(\frac{K_1}{H}, \frac{K_2}{K_1}, \frac{UH}{\nu}\right)$$

and

$$[11] \qquad \frac{u_{0.5}}{U} = \phi\left(\frac{K_1}{H}, \frac{K_2}{K_1}, \frac{UH}{\nu}\right)$$

When the flow is rough turbulent, viscosity should be unimportant and one can expect the velocity distribution to be governed by only two dimensionless variables - the roughness ratio of the two boundaries and the relative roughness of one of the boundaries.

Five values for the roughness ratio K_2/K_1 were chosen, varying from 1.0 to zero. For each value of K_2/K_1, the relative roughness K_1/H was varied from 0.001 to 0.10. For the cases which are expected to be fully turbulent, the depth was kept constant at 2 metres, the unit discharge was maintained at about 0.8 m^2/s; and the Reynolds number UH/ν was about 8×10^5. Several runs were also made in which the roughness ratios were kept fixed and only the Reynolds number was varied.

When one of the boundaries is smooth, i.e. $K_2/K_1 = 0$, the effect of Reynolds number cannot be neglected and the velocity distribution depends on both K_1/H and UH/ν. The effect of Reynolds number on these flows was investigated by varying the Reynolds number and keeping K_1/H cosntant.

A total of 50 flows were calculated. The flow conditions are listed in Table 1.

Results

The variables which were obtained from the calculated velocity distributions are listed in Table 1. In these flows, the rougher of the two boundaries was always taken to be at y=0. Therefore, referring to Fig. 2, y_{max} is the distance from the rougher boundary to the point of maximum velocity; $u_{.2}$ is the velocity two-tenths of the depth away from the smoother boundary; $u_{.8}$ is the velocity two-tenths of the depth away from the rougher boundary; and $u_{.5}$ is the velocity at mid-depth. Considering the flow to be separated into two layers by the line of maximum velocity, U_1 is the average velocity in the layer with the rougher wall and U_2 is the average velocity in the layer with the smoother wall.

Velocity Distribution

In flows number 1 to 5, K_1/H and K_2/K_1 were kept constant at 0.01 and 0.5 respectively. The Reynolds number UH/ν was varied from 7.9×10^5 to 5.0×10^4. The calculated velocity distributions, non-dimensionalized with the mean velocities, are practically identical, as are the calculated variables which are shown in Table 1. Therefore, when the flow at both boundaries are fully rough, the Reynolds number, as expected, has no effect on the velocity distribution.

When one of the walls is smooth, the Reynolds number will have an effect. In flows 38 to 42, K_1/H was kept constant at 0.1 and the Reynolds

number was varied from 7.9×10^5 to 2.0×10^4 by varying either the depth or the mean velocity. Two of these distributions are shown in Fig. 3 and clearly show the change in the velocity profile as the Reynolds number changes. The position of maximum velocity shifts towards the smooth boundary as the Reynolds number increases. There is a much greater change in the velocity profile near the smooth wall as compared to the change near the rough wall. The reason is that the change in Reynolds number has little effect on the friction factor of the rough wall but affects the friction factor of the smooth wall significantly.

Also shown in Fig. 3 is the velocity distribution for flow number 12 in which $K_2/K_1 = 1.0$. Predictably, the profile is symmetrical about $y/H = 0.5$. Together, these profiles in Fig. 3 show that there can be large variations in the velocity distributions under ice-covered rivers, depending on the flow and boundary conditions.

In all the two-layer models of flow under ice cover, the velocity distribution is assumed to be logarithmic in each layer up to the point of maximum velocity. This assumption is not entirely satisfactory because the resulting velocity distribution will have a cusp at the point of maximum velocity. This in itself is not too important but it leads to more serious deficiencies as far as the eddy viscosity and diffusivity distributions are concerned (Lau and Krishnappan 1981). In Fig. 4, the velocities in each layer, non-dimensionalized with the maximum velocity, are plotted against the distances from the wall. It can be seen that the profiles are logarithmic only for about 60 percent of the thickness of each layer. For

the 40 percent of the layer thickness near the location of the maximum velocity, the velocity is less than that given by the logarithmic profile. Only two flows are shown in Fig. 4 but the others all have the same behaviour.

Measurement of Average Velocity

It can be seen from Table 1 that $u_{.2}$ is always larger than the mean velocity U and $u_{.8}$ is always smaller, except for flows with $K_2 = K_1$ when the velocity distribution is symmetrical about y=0.5H. The biggest difference occurs when one wall is smooth and the other has a large relative roughness as in the case of flow number 38 when $u_{.2}$ is 17 percent larger than U and $u_{.8}$ is 13 percent less. Surprisingly, these differences always compensate for each other and the average of the velocities at 0.2 and 0.8 depths are always very close to the mean velocity. For the fifty flows listed, there were three flows in which the error from this procedure is three percent; for all the rest the errors were only about one or two percent. This result could not have been predicted at the outset because the only condition imposed by the model is that the velocity at the grid point closest to the wall is given by the law of the wall. Nevertheless, this shows that the practice of averaging the velocity measurements at 0.2 and 0.8 depths should give a true indication of the average velocity.

The velocity at mid-depth varies from 1.07 to 1.21 times the average velocity. Therefore, the correction coefficient to be applied in order to obtain the average velocity varies from 0.93 to 0.83. The coefficient of

0.88 which is normally used is midway between these values. In Fig. 5, the correction coefficient for all the flows with rough walls are plotted versus K_1/H. It can be seen that the roughness ratio K_2/K_1 is important only when the relative roughness K_1/H is large. For K_1/H less than 0.01, the correction coefficients are larger than 0.88 and are not too much affected by K_2/K_1. Even though the roughness of the ice is not known a priori, Fig. 5 can be used to give a better indication of what the value of the correction coefficient should be. For instance, if the bed roughness is not too large and the ice seems relatively smooth, a correction coefficient of about 0.91 will be more appropriate. If both the river bed and the ice are very rough, a smaller value such as 0.84 will be more correct.

Position of the Maximum Velocity

The values of y_{max}/H listed in Table 1 gives the thickness of the layer adjacent to the rougher boundary and the location of the point of maximum vleocity. This information is important for many of the equations for ice cover roughness and it is interesting to see how it varies with the different flow variables.

In Fig. 6, the values of y_{max}/H are plotted against K_1/H with K_2/K_1 as a parameter. The data from flow numbers 6 to 31 are used to produce the four curves for K_2/K_1 values of 1.0, 0.5, 0.1 and 0.05 respectively. These flows are in the range where the velocity distribution is independent of the Reynolds number. It can be seen from Fig. 6 that y_{max}/H depends

largely on the roughness ratio K_2/K_1 and is only very slightly affected by the relative roughness K_1/H. For K_2/K_1 =0.1, a fifty-fold increase in K_1/H from 0.002 to 0.10 only changed y_{max}/H from 0.60 to 0.64.

A curve for K_2/K_1 =0 is also shown in Fig. 6, based on flow numbers 32 to 37. This shows a much more prominent increase of y_{max}/H with K_1/H. However, it should be noted that this curve is only valid for the Reynolds number value of 8.0×10^5.

The effect of Reynolds number when one wall is smooth is shown in Fig. 7. As expected, Y_{max}/H increases with increase in Reynolds number, largely because of the drop in flow resistance of the smooth wall. When the Reynolds number decreases to 10^5 and the relative roughness decreases to 0.001, the flow resistance of the smooth and rough boundaries are practically the same and the velocity distribution becomes symmetrical, with y_{max}/H equal to 0.5.

Ismail and Davar (1978) measured y_{max}/H for the case of K_1/K_2=0 and a constant Reynolds number. Comparison with the present calculations is difficult because rectangular roughness strips were used and it is not known what the equivalent sand roughness of the surface was. It was also not stated how the Reynolds number was defined. Gogus and Tatinclaux (1981) also measured y_{max}/H in flows with artificial roughnesses. Again, direct comparison with their results is not possible because only the absolute roughness values were presented. However, the trends indicated are the same as in Fig. 7.

Mean Velocities in Top and Bottom Layers

One of the basic assumptions which is often used in the analysis of flow under floating covers is that the mean velocities in the top and bottom layers are equal to each other and to the overall average velocity. The accuracy of this assumption can be examined by using the calculated velocity distributions where the position of maximum velocity can be determined quite accurately.

Using graphical integration, the mean velocities U_1 and U_2 in the layers adjacent to the rougher and smoother walls respectively are evaluated and non-dimensionalized with the overall mean velocity U. Values of U_1/U and U_2/U are listed in Table 1.

It can be seen from Table 1 that U_1/U remains almost constant through changes in K_1/H and changes only very slightly when the roughness ratio K_2/K_1 is altered. Its value is always very close to but slightly less than unity. Even for the flow with one smooth wall together with a wall of fairly large relative roughness ($K_1/H=0.10$), U_1 is only 3 percent less than U.

The mean velocity in the smoother layer, U_2, is always greater than the overall mean and the difference is greater than for the rougher layer, expecially if K_2/K_1 is small. U_2/U increases as K_1/H increases or as K_2/K_1 decreases. When $K_2/K_1=0$, U_2/U also increases with Reynolds number. The largest value of U_2/U_1 in these flows is 1.09, which occurred when $K_2/K_1=0$, $K_1/H=0.10$ and $UH/\nu=8\times10^5$. For this flow, $U_1/U=0.97$ and

the difference between U_1 and U_2 is about 12 percent. In general, unless the difference between the roughnesses of the two boundaries is very large, the mean velocity in the smoother layer should be greater than the mean velocity in the rougher layer by not more than 5 percent. Therefore, the assumption that the mean velocities are equal in the two layers may be acceptable for most uniform ice covers.

Conclusions

Using the k-ε turbulence model, velocity distributions for channel flows with floating covers have been calculated. The distributions have been used to examine the behaviour of some of the variables which are significant for the study of flow under ice covers. These calculations are performed for uniform flow conditions and should be valid for normal ice-covered flows. Other conditions, such as the flow just downstream of a large ice jam, may produce different distributions.

The computed velocity distributions show that the velocity profiles are logarithmic only for about 60 percent of the layer thickness. For the 40 percent of the flow near the location of maximum velocity, the velocities are less than that given by the logarithmic distribution.

The velocities at 0.2 and 0.8 depths may deviate significantly from the overall average velocity. However, the differences seem to compensate for each other and the average of these two velocities is only about 2 percent higher than the actual mean velocity for most of the flows

considered. This result lends confidence to the two-point method for flow gauging.

When the depth is small and the velocity has to be measured at mid-depth, the correction coefficient needed to obtain the mean velocity can be 5 percent larger or smaller than the value of 0.88 which is generally used. Fig. 5 can be used as a rough guide to select a better correction coefficient.

The distance to the point of maximum velocity or the thickness of the rougher layer increases as the difference in the roughness of the boundaries increases. For fully rough flow, this thickness is almost independent of the relative roughness K_1/H. However, when one boundary is smooth or when the flow near the boundary is not fully rough, both the Reynolds number and the relative roughness can have an appreciable effect. The effect of K_2/K_1 and K_1/H follows the same trend as found by Gogus and Tatinclaux (1981). The effect of Reynolds number has not been investigated in previous studies.

The mean velocities in the top and bottom layers are, in most cases, within 5 percent of each other. The assumption that these two velocities are equal will not be too much in error except when the difference between the boundary roughnesses is large, say $K_2/K_1 < 0.1$, and $K_1/H \geq 0.1$.

Acknowledgments

The author wishes to thank Spyros Beltaos for many helpful discussions. The empirical expression for B_s in Eq. 9 was kindly provided by M. S. Yalin.

References

GOGUS, M., and TATINCLAUX, J.C. 1981. Characteristics of flow below a rough floating cover. Proceedings of Workshop on Hydraulic Resistance of River Ice, National Water Research Institute, Burlington, Ontario, pp. 122-141.

ISMAIL, E., and DAVAR, K. S. 1978. Resistance to channel flow under a very rough top boundary. Proceedings of IAHR Symposium on Ice Problems, Part II, pp. 435-447, Lulea, Sweden.

LAU, Y. L., and KRISHNAPPAN, B. G. 1981. Ice cover effects on stream flows and mixing. ASCE Journal of the Hydraulics Division, Nov. 81,(in press).

LAUNDER, B. E., and SPALDING, D. B. 1974. The numerical calculation of turbulent flows. Computer Methods in Applied Mechanics and Engineering, Vol. 3, pp. 269-289.

PRATTE, B. 1979. Review of flow resistance of consolidated, smooth, and rough ice covered waters. Canadian Hydrology Symposium, May 10-11, 1979, Vancouver.

RASTOGI, A. K., and RODI, W. 1978. Predictions of heat and mass transfer in open channels. ASCE Journal of the Hydraulics Division, 104 (HY 3).

RODI, W. 1978. Turbulence models and their application in hydraulics - a state-of-the-art review. Technical Report No. SFB 80/T/127, University of Karlsruhe, Karlsruhe, Germany.

YALIN, M. S. 1972. Mechanics of sediment transport. Pergamon Press, pp. 28.

Tables

TABLE 1. Flow Conditions and Derived Variables

No.	H cm	U cm/s	K_1 cm	K_2 cm	$\frac{K_1}{H}$	$\frac{K_2}{K_1}$	$\frac{UH}{\nu}$	$\frac{Y_{max}}{H}$	$\frac{u_{.5}}{U}$	$\frac{u_{.2}}{U}$	$\frac{u_{.8}}{U}$	$\frac{u_{.2}+u_{.8}}{2U}$	$\frac{U_1}{U}$	$\frac{U_2}{U}$
1	200	39.9	2.0	1.0	0.01	0.5	7.9×10^5	0.53	1.12	1.03	0.99	1.01	0.99	1.01
2	100	39.9	1.0	0.5	0.01	0.5	4.0×10^5	0.54	1.12	1.03	0.99	1.01	0.99	1.01
3	50	39.9	0.5	0.25	0.01	0.5	2.0×10^5	0.54	1.12	1.03	0.99	1.01	0.99	1.01
4	25	39.9	0.25	0.125	0.01	0.5	1.0×10^5	0.53	1.12	1.03	0.99	1.01	0.99	1.01
5	12.5	39.9	0.125	0.063	0.01	0.5	5.0×10^4	0.54	1.12	1.03	0.99	1.01	0.99	1.01
6	200	40.1	0	0	0	1.0	8.0×10^5	0.50	1.07	1.03	1.03	1.03	1.00	1.00
7	200	40.0	0.2	0.2	.001	1.0	8.0×10^5	0.50	1.09	1.01	1.01	1.01	1.00	1.00
8	200	40.0	0.4	0.4	.002	1.0	8.0×10^5	0.50	1.10	1.01	1.01	1.01	1.00	1.00
9	200	39.9	1.2	1.2	.006	1.0	8.0×10^5	0.50	1.12	1.01	1.01	1.01	1.00	1.00
10	200	39.8	2.0	2.0	.010	1.0	8.0×10^5	0.50	1.13	1.01	1.01	1.01	1.00	1.00
11	200	39.7	4.0	4.0	.020	1.0	7.9×10^5	0.50	1.15	1.01	1.01	1.01	1.00	1.00
12	200	39.6	6.0	6.0	.030	1.0	7.9×10^5	0.50	1.16	1.01	1.01	1.01	1.00	1.00
13	200	39.2	20.0	20.0	.100	1.0	7.8×10^5	0.50	1.21	1.01	1.01	1.01	1.00	1.00
14	200	40.0	0.2	0.1	.001	0.5	8.0×10^5	0.53	1.09	1.02	0.99	1.01	0.99	1.01
15	200	40.0	0.4	0.2	.002	0.5	8.0×10^5	0.53	1.10	1.02	0.99	1.01	0.99	1.01
16	200	39.9	1.2	0.6	.006	0.5	8.0×10^5	0.53	1.11	1.03	0.99	1.01	0.99	1.01
17	200	39.9	2.0	1.0	.010	0.5	8.0×10^5	0.53	1.12	1.03	0.99	1.01	0.99	1.01
18	200	39.8	4.0	2.0	.020	0.5	8.0×10^5	0.54	1.14	1.03	0.99	1.01	0.99	1.01
19	200	39.7	6.0	3.0	.030	0.5	7.9×10^5	0.54	1.15	1.04	0.98	1.01	0.99	1.02
20	200	39.3	20.0	10.0	.100	0.5	7.9×10^5	0.54	1.17	1.05	0.98	1.02	0.99	1.03
21	200	40.0	0.4	0.04	.002	0.1	8.0×10^5	0.60	1.09	1.02	0.97	1.00	0.99	1.02
22	200	39.9	1.2	0.12	.006	0.1	8.0×10^5	0.60	1.09	1.06	0.96	1.01	0.99	1.03
23	200	39.9	2.0	0.20	.010	0.1	8.0×10^5	0.60	1.10	1.06	0.96	1.01	0.98	1.03
24	200	39.8	4.0	0.40	.020	0.1	8.0×10^5	0.61	1.11	1.07	0.95	1.01	0.98	1.03
25	200	39.7	6.0	0.60	.030	0.1	7.9×10^5	0.62	1.12	1.08	0.94	1.01	0.98	1.04
26	200	39.3	20.0	2.00	.100	0.1	7.9×10^5	0.64	1.15	1.12	0.92	1.02	0.98	1.06
27	200	39.9	1.2	0.06	.006	0.05	8.0×10^5	0.63	1.09	1.07	0.95	1.01	0.98	1.03
[illegible]	200	39.9	2.0	0.10	.010	0.05	8.0×10^5	0.63	1.09	1.08	0.95	1.02	0.98	1.04

TABLE 1. Flow Conditions and Derived Variables cont'd.

Flow No.	H cm	U cm/s	K_1 cm	K_2 cm	$\frac{K_1}{H}$	$\frac{K_2}{K_1}$	$\frac{UH}{\nu}$	$\frac{Y_{max}}{H}$	$\frac{u_{.5}}{U}$	$\frac{u_{.2}}{U}$	$\frac{u_{.8}}{U}$	$\frac{u_{.2}+u_{.8}}{2U}$	$\frac{U_1}{U}$	$\frac{U_2}{U}$
29	200	39.7	4.0	0.20	.020	0.05	7.9×10^5	0.64	1.10	1.09	0.94	1.02	0.98	1.04
30	200	39.7	6.0	0.30	.030	0.05	7.9×10^5	0.65	1.11	1.10	0.93	1.02	0.99	1.04
31	200	39.3	20.0	1.00	.100	0.05	7.9×10^5	0.66	1.14	1.14	0.91	1.03	0.97	1.07
32	200	40.0	0.2	0	.001	0	8.0×10^5	0.58	1.08	1.04	0.98	1.01	0.99	1.02
33	200	40.0	0.4	0	.002	0	8.0×10^5	0.61	1.08	1.05	0.97	1.01	0.99	1.02
34	200	39.9	1.2	0	.006	0	8.0×10^5	0.66	1.08	1.08	0.95	1.02	0.98	1.04
35	200	39.8	2.0	0	.010	0	8.0×10^5	0.67	1.08	1.10	0.93	1.02	0.98	1.05
36	200	39.7	4.0	0	.020	0	7.9×10^5	0.72	1.09	1.12	0.92	1.02	0.98	1.06
37	200	39.6	6.0	0	.030	0	7.9×10^5	0.74	1.09	1.13	0.91	1.02	0.98	1.07
38	80	98.3	8.0	0	0.100	0	7.9×10^5	0.79	1.09	1.17	0.87	1.02	0.97	1.09
39	20	98.4	2.0	0	0.100	0	2.0×10^5	0.77	1.10	1.17	0.87	1.02	0.97	1.08
[illegible]	20	49.3	2.0	0	0.100	0	9.9×10^4	0.74	1.11	1.16	0.88	1.02	0.97	1.08
[illegible]	100	9.9	10.0	0	0.100	0	9.9×10^4	0.74	1.11	1.16	0.88	1.02	0.96	1.08
42	20	9.9	2.0	0	0.100	0	2.0×10	0.69	1.12	1.15	0.90	1.03	0.97	1.06
43	200	39.8	2.0	0	.010	0	8.0×10^5	0.67	1.08	1.10	0.93	1.02	0.98	1.05
44	50	39.9	0.5	0	.010	0	2.0×10^5	0.65	1.09	1.08	0.95	1.02	0.98	1.02
45	25	39.9	0.25	0	.010	0	1.0×10^5	0.62	1.10	1.07	0.96	1.02	0.99	1.02
46	5	39.9	0.05	0	.010	0	2.0×10^4	0.54	1.11	1.03	0.99	1.01	0.99	1.01
47	200	40.0	0.2	0	.001	0	8.0×10^5	0.58	1.08	1.04	0.98	1.01	0.99	1.02
48	50	40.1	0.05	0	.001	0	2.0×10^5	0.53	1.09	1.02	1.00	1.01	1.00	1.00
49	25	40.1	0.025	0	.001	0	1.0×10^5	0.50	1.09	1.01	1.01	1.01	1.00	1.00
50	20	10.1	0.020	0	.001	0	2.0×10^4	0.50	1.11	1.01	1.01	1.01	1.00	1.00

Figures

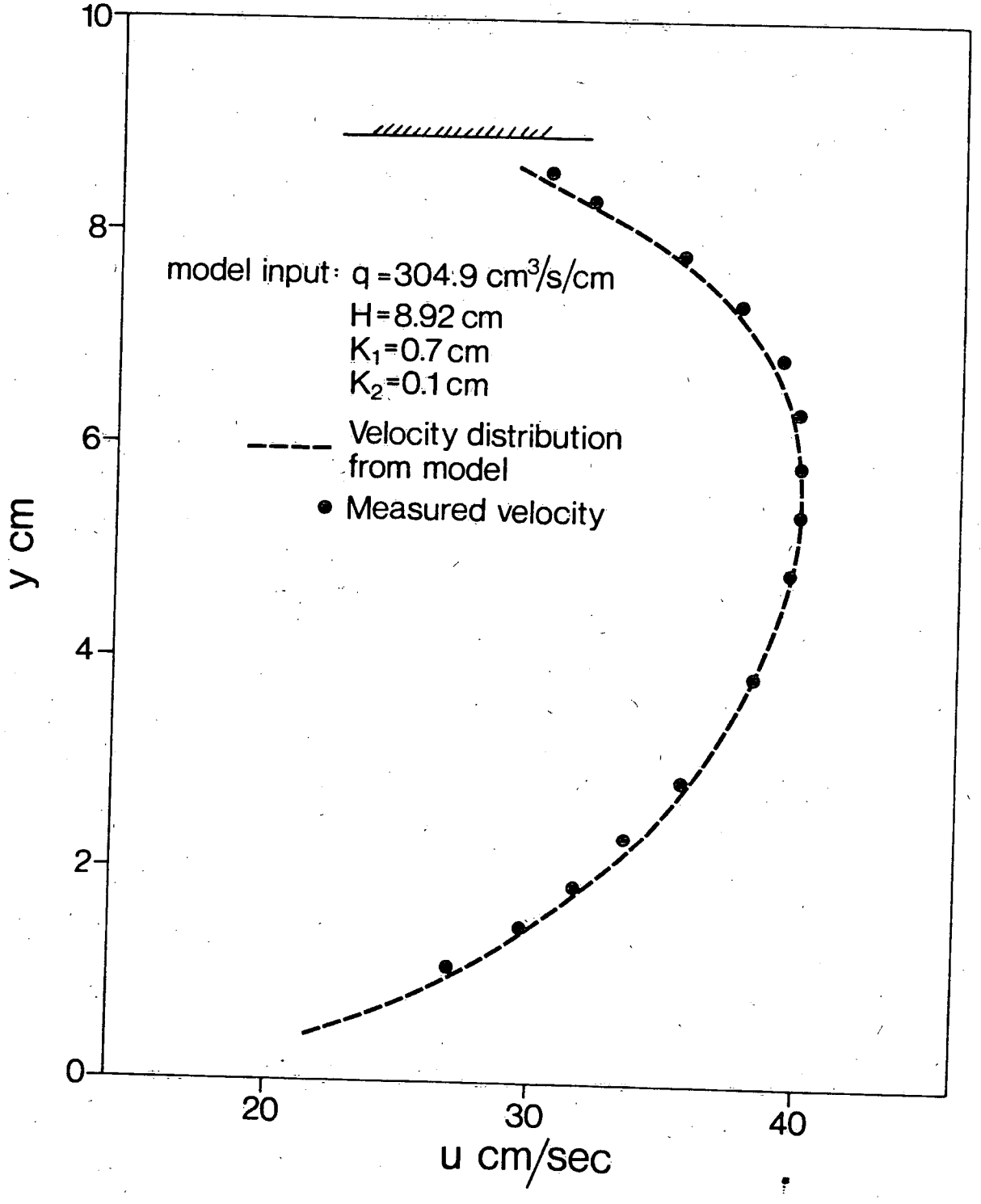

Figure 1 Comparison of turbulence model output and measured velocity distribution

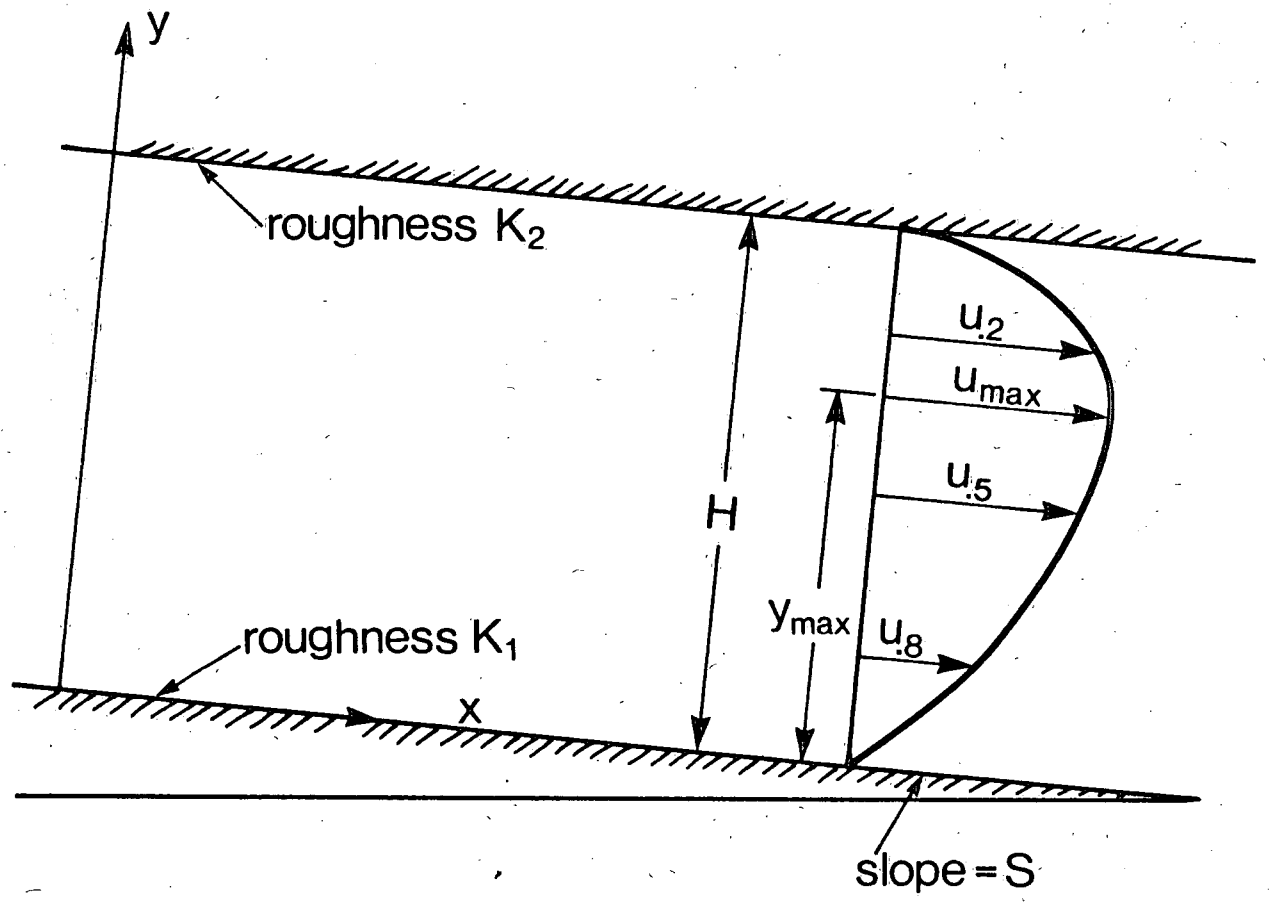

Figure 2 Definition sketch

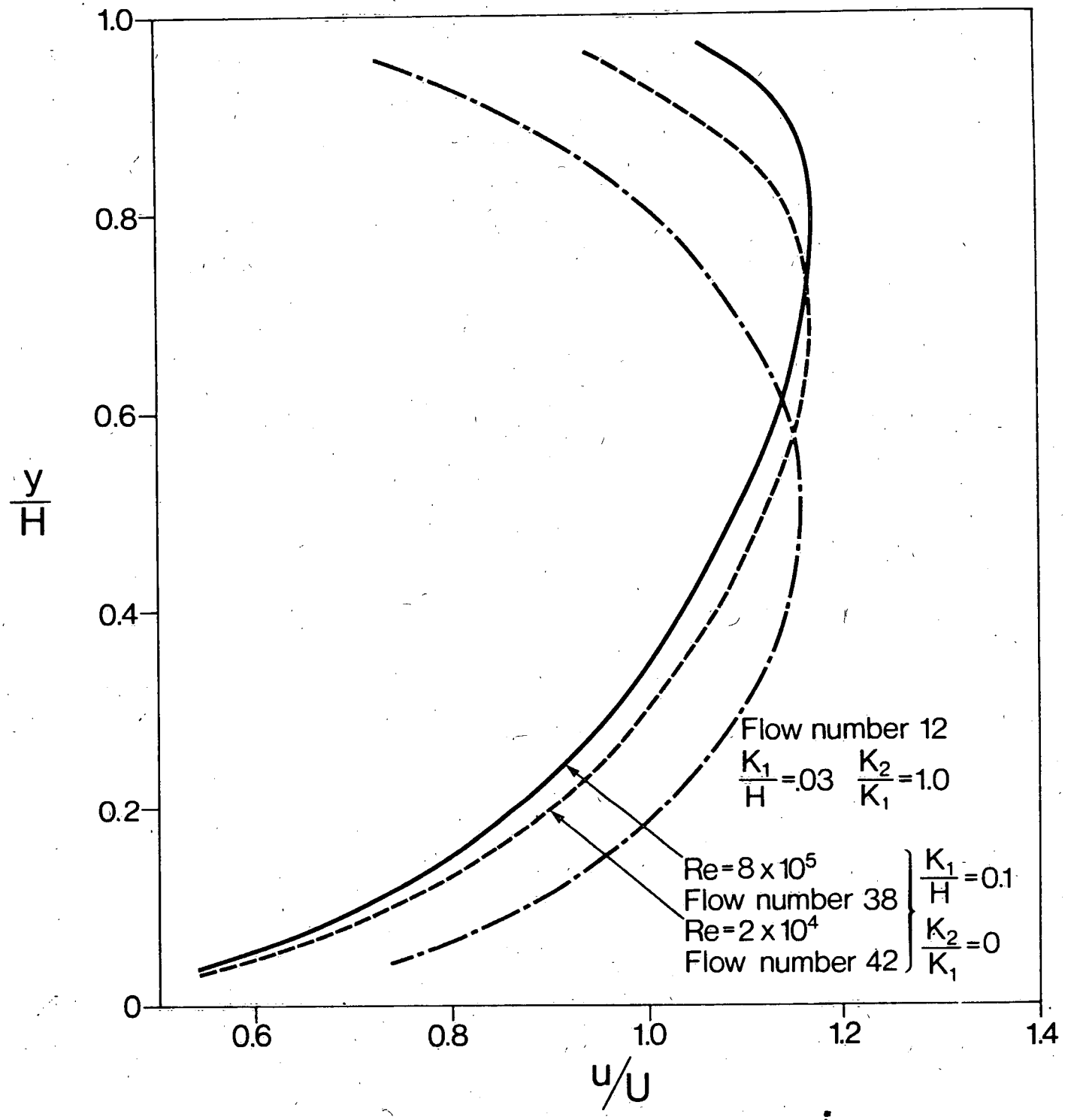

Figure 3 Effect of Reynolds number and boundary roughnesses on velocity distribution

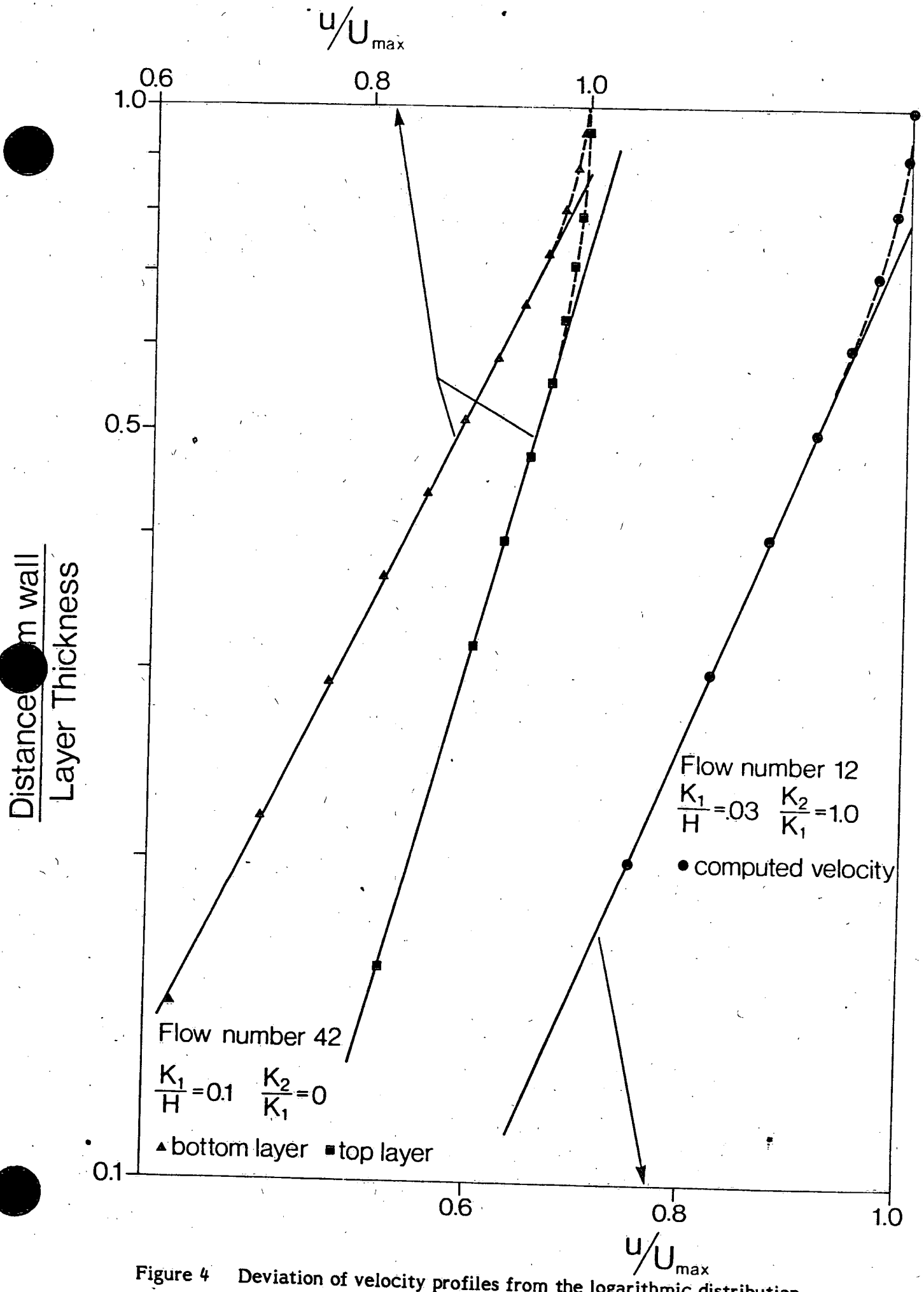

Figure 4 Deviation of velocity profiles from the logarithmic distribution

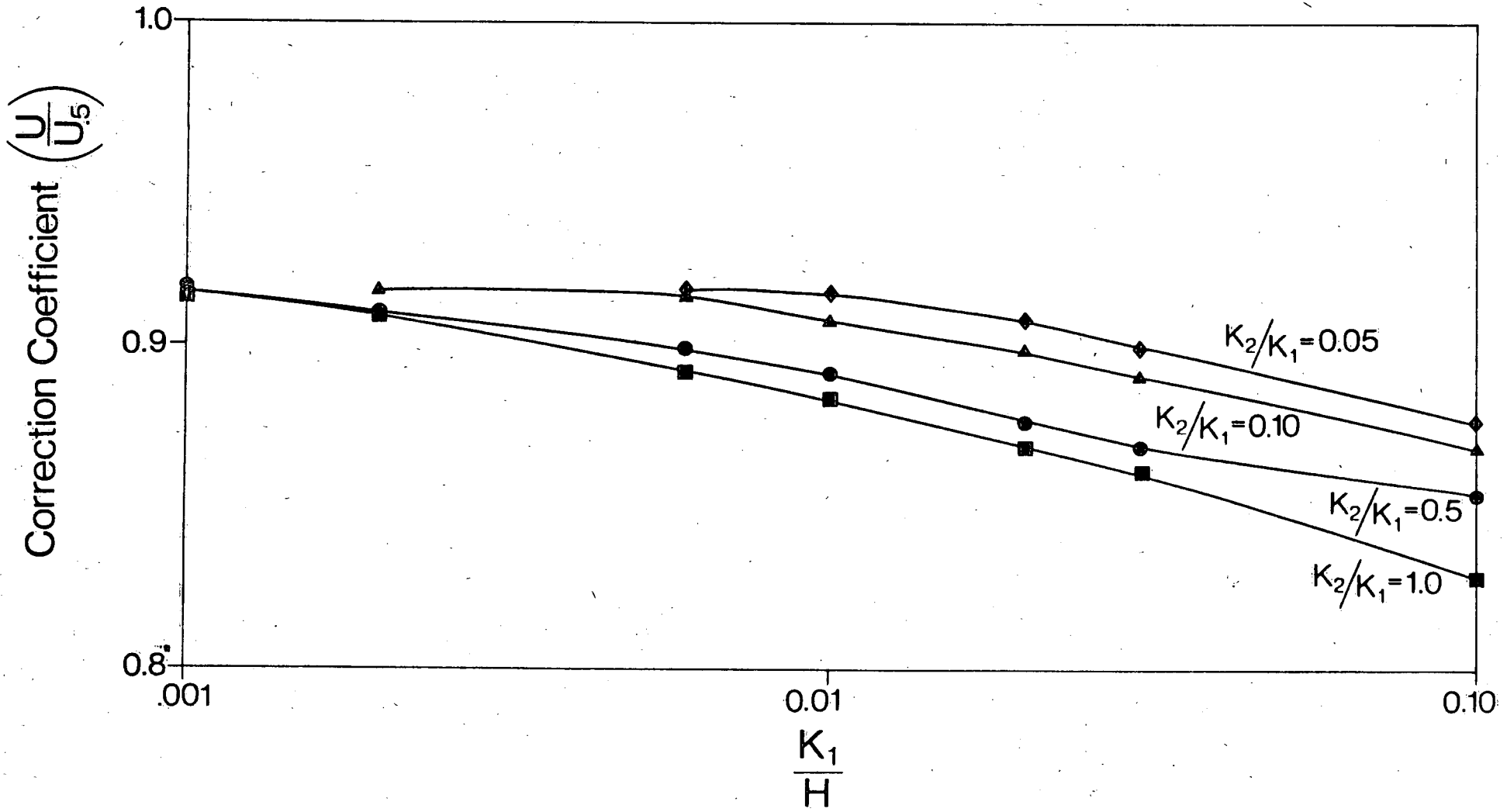

Figure 5 Variations of the correction coefficient with K_1/H and K_2/K_1

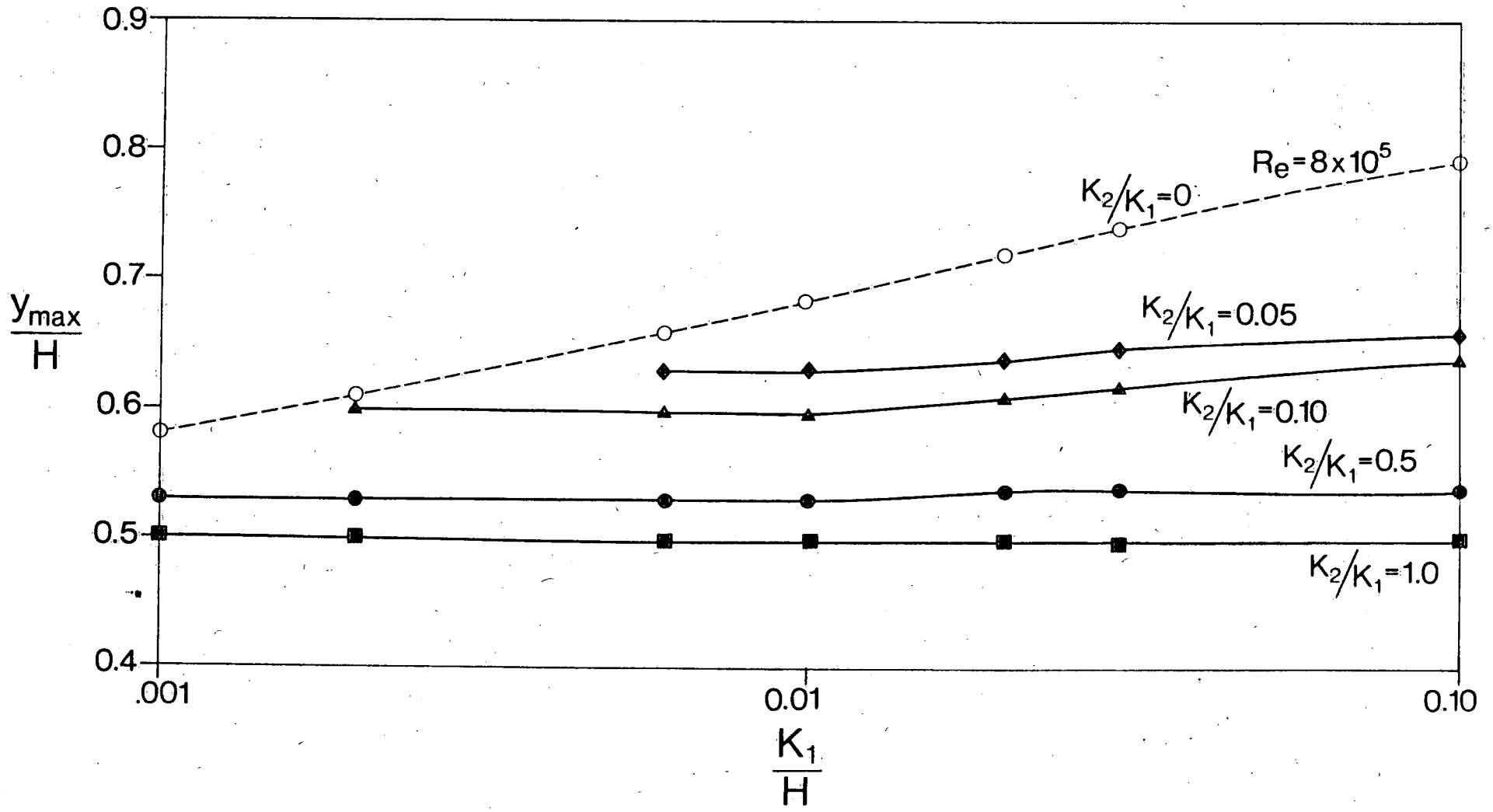

Figure 6 Variations of the location of maximum velocity

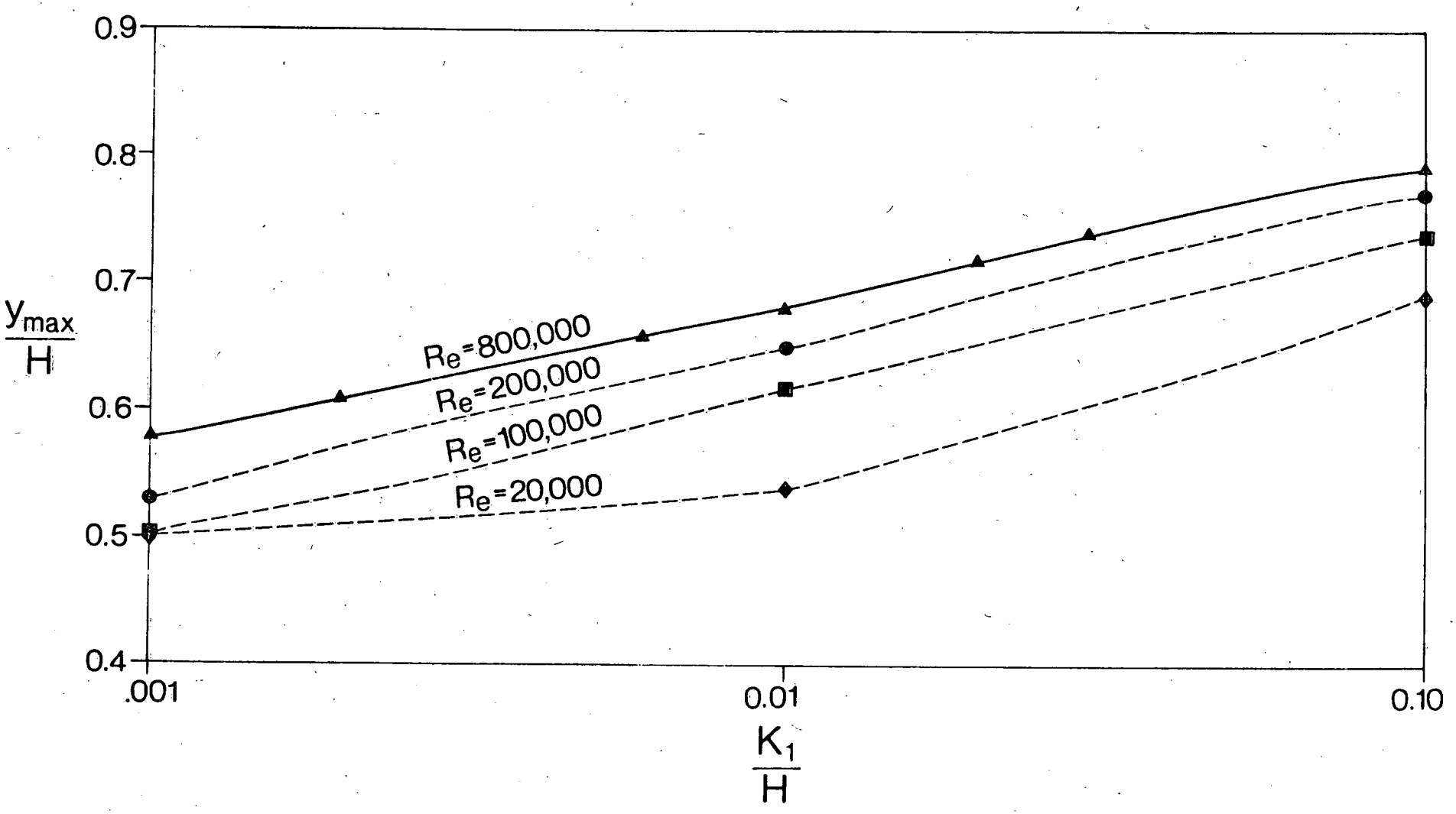

Figure 7 Effect of Reynolds number on the location of maximum velocity when one wall is smooth